Numerical Simulation for the Impact of Deforestation on Climate in China and Its Neighboring Regions

Song Yukuan (宋玉宽), *Chen Longxun* (陈隆勋) and *Dong Min* (董 敏)
Chinese Academy of Meteorological Sciences, SMA, Beijing 100081
Received May 8, 1993; revised December 8, 1993

ABSTRACT

In this paper, the CCM0B model is used to study the effect of the deforestation on the climate of China and its neighboring regions. On the assumption that the forest in China would be replaced by the vegetation(such as grassland), the distribution of the albedo changed was calculated. The initial fields used were taken from the FGGE zonal mean data on 16 July, 1979. In the control simulation, the observed albedo data were used to modify the physical parameters of the original model. The control and sensitive experiments were run each for 210 days, in which the external forcing fields were fixed in July. As a result, we find that the East Asian Monsoon, Hadley cell and troposphere easterly jet are weakened for the deforestation in China. The precipitation and cloud amount over China are also decreased. The changes in evaporation and surface temperature are small. The results also show that the deforestation in China exerts a remarkable effect on the climate in the neighboring regions of China.

Key Words: Numerical simulation, Deforestation, Climate model

I. INTRODUCTION

The climate change for the worse, caused by the deforestation, is one of the ten most serious environmental crises resulted from the human activities. Many scientists began to study the effects of the deforestation on the climate as early as in 1970s. After analyzing satellite radiation data, Otterman (1974) pointed out that the increasing of surface albedo for the destruction of vegetation and the exposure of the land could lead to the decrease of the solar radiation absorbed by the surface land, consequently, the surface soil temperature became lower, and the weakening of latent heat exchange impelled the atmospheric convective precipitation to decreasing. There was somebody who made an objection against this point of view and pointed out that, with the increasing of reflection of the short wave radiation, the surface upward long wave radiation would also be decreased simultaneously. So the surface temperature increased slightly sometimes. Charney (1975a) used the dynamics method to study the impacts of the increasing of albedo in North Africa on climate in order to explain the formation of Sahara desert.

Charney (1975b) also used the GISS GCM to do further simulation for the effect of albedo by increasing it from 15% to 35%, the results showed that the precipitation decreased remarkably. The simulation experiments for Dust Bowl and Thar of the United States obtained the similar results. Charney et al.(1977) proposed that the increasing of albedo would suppress evapotranspiration and consequently reduce the local convective precipitation. Suel et al. (1982) used the GLAS GCM to validate Charney's results again. They verified this result and pointed out that the similar climatic influence could be found in the northeast part of Brazil. Assuming that the tropical rainforest in Amazon River Valley of South America had been replaced by grassland, Dickinson et al. (1988) studied the interactions between forest and climate by using NCAR CCM coupled with a biosphere– atmospheric model. The

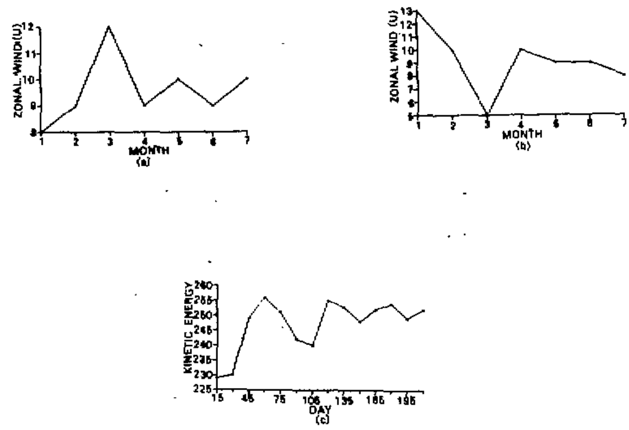

Fig. 1. The distribution of the 1s-day averaged kinetic energy at 200 hPa.

results showed that the precipitation and evaporation decreased, while the surface temperature went up. The precipitation decreased by 1.3 mm / day.

The above-mentioned experiments researched the effects of deforestation on the climate in Sahara, Amazon River Valley et al., however, the studies on deforestation in China with the GCM have not been conducted up to now. But the similar experiments have been carried with some simple models in China. The desert and arid area in China accounts for about 15.5% of this country, which is increasing in the speed of 1560 kilometers each year. The influence of the deforestation on the drought was great. The Chinese scientists should do much resaerch work on this issue.

In this paper, the nine-level global climatic model NCAR CCM0B was used to study the effects of deforestation on the climate of China and its neighboring regions. The results show that the deforestation in China influences not only the climate of China but also that of its neighboring regions.

II. DESCRIPTION OF MODEL AND DESIGN OF EXPERIMENT

The NCAR CCM0B model is a nine-level global climatic model with 15-wave rhomboidal truncation. The details of the model are referred to the NCAR Technical report(Williamson, 1989).

The initial fields used in the experiment were taken from the FGGE data set at 00 am 16 July, 1979, which were analyzed and sorted out by ECMWF. In July, the physical parameters of the surface layer, except the vegetation, the type of forest and the relevant albedo in China, were cited from the NCAR CCM1 model(for example, SST et al.).

We calculated the 15-day averaged kinetic energy at 200 hPa in order to examine the time when the integration would approach to equilibrium state. We ran the model each for seven months with two different initial fields: one was taken from the FGGE data set of the global grid points on 16 July, 1979(the values, on the grid points $1.875° \times 1.875°$, were interpolated into the grid point $4.35° \times 7.5°$used in CCM0B); another initial field was taken from the zonal mean data. The results of 210-day integration show that the kinetic energy which was calculated in the simulation with the initial field coming from the zonal mean data approaches to equilibrium state quickly after four months (Fig. 1), while there still are some oscillations in the former integration. In the later experiment, the inter-monthly variations of the circulation are also very small after four months. This proves that the results obtained from Fig. 1 are reliable. Recently, in another experiment, the later integration is continuously run for another four months, then we find that the inter-monthly oscillations of integration are very small. The initial fields used in the following experiments were taken from the zonal mean data.

We made two experiments for contrast, one is the control experiment and another the sensitive experiment. In the control experiment, the albedo values used in the model were taken from the albedo data sets given by Mathews (1985), which were interpolated into the grid point $5^\circ \times 5^\circ$from the origional grid point $1^\circ \times 1^\circ$. The distribution of the albedo in China is shown in Fig. 2a. In the sensitive experiment, we assumed that all the forest in China were destroyed, one part of which were replaced with grassland, another part of which were replaced with the bare land. For this reason, the albedo values of the deforestation are not simply the bare land's. We calculated the albedo of the deforestation in China with the following empirical formula:

$$A = AF \times AC + AA \times (1 - AC) \ .$$

Where A is the real albedo used in the control exeperiment, AF is the forest albedo, AA is the combination albedo of the vegetation and bare land, AC is the covering ratio of forest. AF was calculated with the different types of the forest which were taken from the map sets of the People's Republic of China (1989). Table 1 shows the albedos for 30 vegetation types. AC was obtained from the statistic values of the covering ratio of forest which were taken from the third investigation data of the forest throughout the country during the period of 1973-1976(1990). Therefore, we calculated the value of AA with the formula mentioned above. On the assumption that the forest were replaced with the vegetation and the uncovered land around the forest, AA was regarded as the albedo of the deforestation in sensitive experiment. Fig. 2b shows the difference of albedo between the sensitive and control experiment.

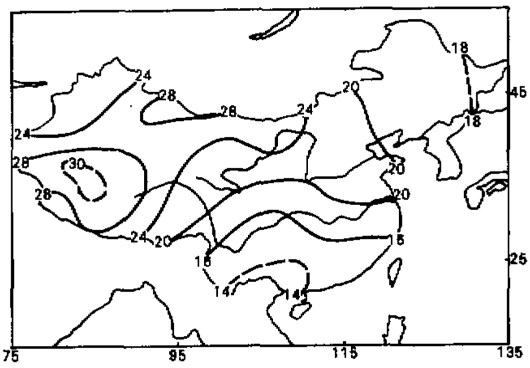

Fig. 2a. The distribution of albedo in China in the control simulation.

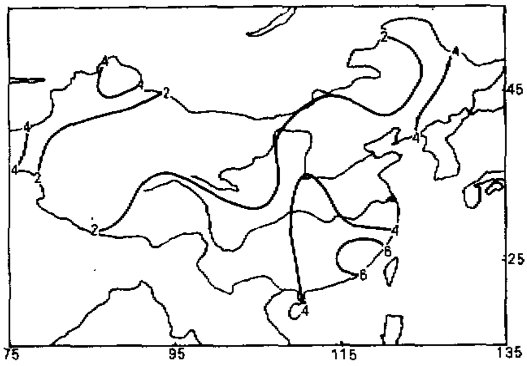

Fig. 2b. The difference of the albedo from the control simulation.

Table 1. Albedos for 30 vegetation types

ALBEDO	DESCRIPTION OF VEGETATION TYPE
11	tropical evergreen rainforest
11	tropical / subtropical evergreen seasonal broadleaved forest
11	subtropical evergreen rainforest
12	temperate / subpolar evergreen rainforest
14	temperate evergreen seasonal broadleaved forest, summer rain
13	evergreen broadleaved sclerophyllous forest, winter rain
16	tropical / subtropical evergreen needleleaved forest
15	temperatre / subpolar evergreen needleleaved forest
15	tropical / subtropical drought–deciduous forest
18	cold–deciduous forest, with evergreens
18	cold–deciduous forst, without evergreens
28	xeromorphic forest / woodland
12	evergreen needleleaved sclerophyllous woodland
16	evergreen needleleaved woodland
17	tropical / subtropical drought–deciduous woodland
17	cold–deciduous woodland
18	evergreen broadleaved shrubland / thicket, evergreen dwarf–shrubland
18	evergreen needleleaved or microphyllous shrubland / thicket
20	drought–deciduous shrubland / thicket
20	cold–deciduous subalpine / subpolar shrubland, cold–deciduous dwarf shrubland
28	xeromorphic shrubland / dwarf shrubland
17	arctic / alpine tundra, mossy bog
17	tall / medium / short grassland with 10–40% woody tree cover
16	tall / medium / short grassland with < 10% woody tree cover or tuft–plant cover
25	tall / medium / short grassland with shrub cover
20	tall grassland, no woody cover
20	medium grassland, no woody cover
20	meadow, short grassland, no woody cover
20	forb formations
30	desert

As shown in Fig. 2a and Fig. 2b, the albedo values in the sensitive experiment increase by 1–6%. On the average, the albedo increases by 2% all over the country, with the highest value in the area east to 95°E and south to 40°N, especially in the area south to the Yangtze River Valley, the albedo values increase by 6% or so. The small changes of the albedo in the northwestern China and the plateau imply that the covering ratio of forest in that region is very small.

III. RESULTS OF THE CONTROL EXPERIMENT

The ability for the control experiment to simulate the main climate features is one of the most important symbols of the successful numerical simulation. So we discuss the results of the control experiment first of all. The fields of wind vectors simulated at 200 hPa and 850 hPa in the control experiment are shown in Fig. 3a and Fig. 3b, which are the averaged results of the integration in seventh month. Because the albedo in China is a real value, the simulation in Asia is better than before. Comparing Fig. 3a and Fig. 3b with the climate maps (Dong Min et al., 1990), we find that the positions of the 200 hPa anticyclones over the Qinghai–Xizang Plateau and the northern Australia simulated near 30°N, 85°E and 15°S, 135°E, are very well as compared with its climatic positions near 28°N, 87°E and 13°S, 137°E. The two branches of upper easterly jet separately locating at the area south to the anticyclone over South Asia and the equator of East Asia are also simulated very well. The troughs and ridges in the high and middle latitudes of the Northern Hemisphere are simulated out. The unsatisfied results are that the simulated anticyclone over Arabia is weak, and the upper troughs over the mid part of North Pacific are not obvious.

At 850 hPa, the southern Asian monsoon extends from Arabic Sea to South China Sea. The Yellow River and the Yangtze River are covered with the troughs. The axis of the subtropic anticyclone over the western Pacific is situated in the area south to the Yangtze River(25°–27°N). These simulated results are in coincidence with the climatic features. In addition, the southeastern Africa of 25°N and the Eastern Australia are occupied by cold anticyclones separately; In the observation, the southern Africa(alone 25°N) and the mid–Australia are dominated by cold anticyclones also, but the position of the simulated Australian anticyclone is to the east and its intensity is weak.

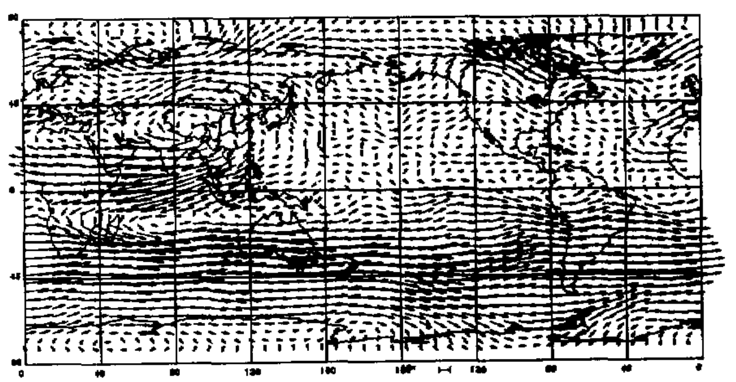

Fig. 3a. The control test wind at 200 hPa.

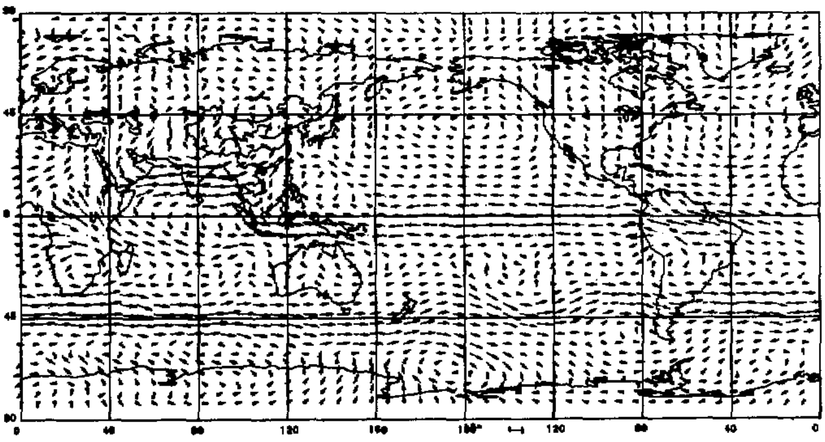

Fig. 3b. The control test wind at 850 hPa.

The precipitation in the control experiment in July is shown in Fig.4. The North China of the lower reaches of the Yellow River, from Shandong Province to the south part of Liaoning Province, exhibits a centre of the precipitation with the central value about 360 mm / month. Besides, the Bay of Bengal is also covered with a strong center of precipitation. In the climatic distribution of the precipitation, a centre of the precipitation with the mean value about 300 mm / month appears in Shandong Province and the east part of Liaoning Province, so the simulated precipitation is similar to the climate state. Guangdong Province is covered by a centre of the precipitation with the central value about 300 mm / month; there is also a centre of the precipitation with the value about 500 mm / month in the south part of Guangxi Province. In addition, in the southwestern China, only the common border of Yunnan Province and the Xizang Autonomous region is dominated by a centre of the precipitation with the value more than 600 mm / month. Comparing with the climate state, the precipitation in North China is simulated well, while the location of the centre of the precipitation in South China is to the east and the position of the centre of the precipitation in the Xizang Autonomous region is to the west. To sum up, the three strong precipitation cells in China in July are simulated out, and their intensities are simulated well, but the positions of two precipitation cells in southern China are not satisfied. The reason may be that the resolution of the model used is low.

IV. RESULTS OF THE SENSITIVE EXPERIMENT

The sensitive experiment and the control experiment are different, because the albedo used in the sensitive experiment was increased due to the deforestation. The increments are shown in Fig. 2b. We discussed the difference of circulations between the sensitive experiment and the control experiment.

1. *Difference of Circulations*

The difference of wind vector between the sensitive experiment and the control experiment at 200 hPa is shown in Fig. 5a. We find that the changes of the albedo in China exert

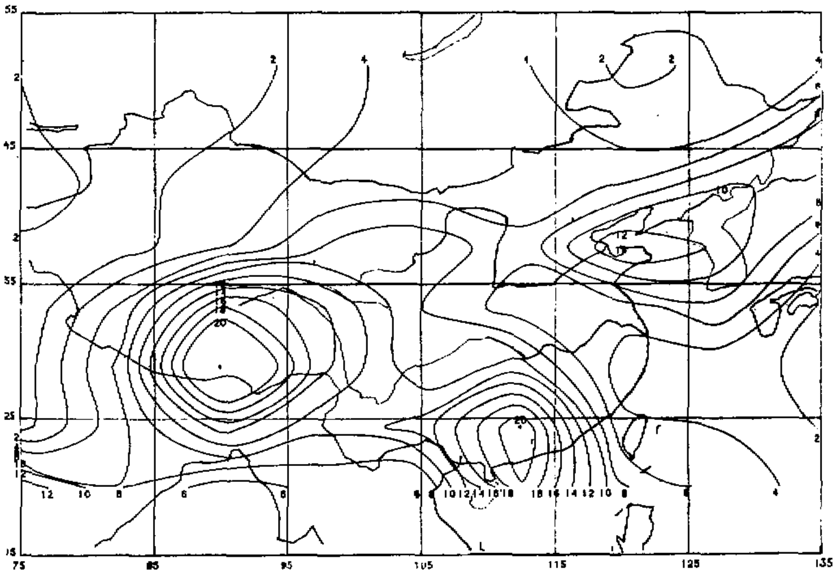

Fig. 4. C-test 7th month China rainfall.

great effects on the atmospheric circulations in the local and its neighboring regions. The results are as follows:

As shown in Fig. 5a, there are two abnormal cyclonic circulations appearing over the region south to the Yellow River and the northwestern China. The most part of the northeastern China are also dominated by the abnormal cyclonic circulations. This indicates that the 200 hPa anticyclonic circulations influencing the climate of China are weakened and the high-level divergences in China are weakened also.

It is shown in Fig.5a that the appearance of an abnormal cyclonic circulation over the northern Arabia and the northwest part of the Persian Gulf implies that the subtropical anticyclonic belt over these regions is weakened. The centre of the westerly jet in the high and middle latitudes of the Northern Hemisphere is located near the region south to this anticyclonic belt, and the centre of the easterly jet over Arabian Sea is found in the north part of this anticyclonic belt. So the appearance of the abnormal cyclonic circulation in the Eastern Hemisphere of 37°N will lead to the weakening of the easterly jet and the westerly jet. Especially the intensity of the easterly jet over the Arabian Sea decreases by 15 m / s. The westerly jet decreases by 4 m / s or so. The weakening of the easterly jet over the Arabian Sea and the appearance of the abnormal anticyclonic circulation over the northern Arabia and the northern Persian Gulf are the results of the weakening of the anticyclone over China. Thus, the changes of the albedo due to the deforestation in China exert a notable influence on the intensity of the easterly and westerly jet.

Over the Pacific Ocean, from 40°N, 180°W to 40°N, 140 °W, an abnormal anticyclonic circulation and an abnormal ridge of the high are observed, this shows that the trough controling this region at 200 hPa is weakened.

It is also shown in Fig.5a that an abnormal cyclone dominates over the Indian Ocean, this indicates that the anticyclone occurring in this region in control simulation is weakened due to the decreasing of the upper easterlies.

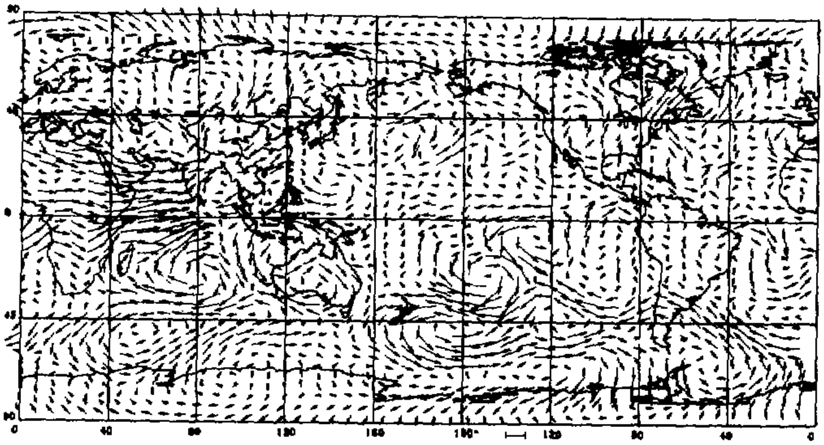

Fig. 5a. The difference of the 200 hPa velocity vector between the sensitive and control experiment.

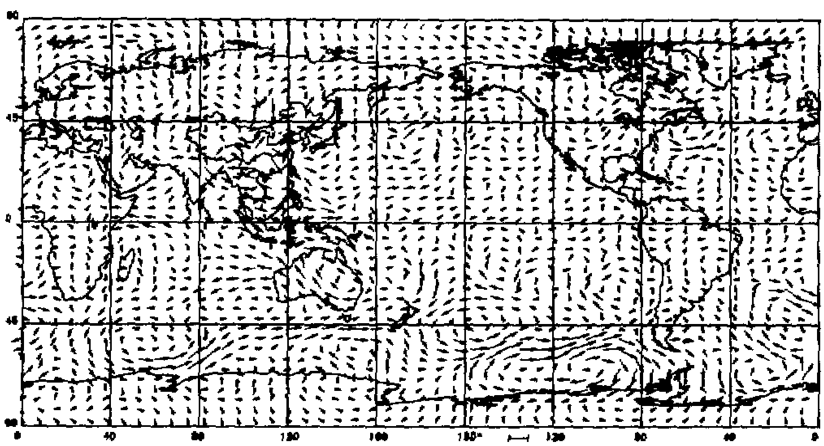

Fig. 5b. The difference of the 850 hPa velocity vector between the sensitive and control experiment.

The abnormal southeast air stream dominates over the area from Indian peninsula to the south part of South China Sea and the western tropical Pacific, this implies that the southern branch of the easterly jet is strengthened. On the contrary, the northern branch of the easterly is weakened.

The difference of wind vector at 850 hPa is shown in Fig.5b. As a result, we find that the change in the albedo of China exerts a great influence on the circulations also. The wave trains of the abnormal cyclone and anticyclone at 850 hPa propagate from China to the Western Hemisphere. The main changes of the circulations are as follows:

Two abnormal anticyclonic circulations are prevailing over the eastern and western part of China, which are corresponding to the abnormal cyclonic circulations at 200 hPa and show that the low-layer divergence is strengthened, while the upper divergence is weakened. Consequently, the ascending motion in the region decreases, and the precipitation decreases also.

Two abnormal cyclonic circulations are found over the Pacific at 850 hPa, which are corresponding to the abnormal anticyclonic circulations at 200 hPa and imply that the subtropic high over the Pacific is weakened. Therefore, the southeastern air stream which is near the south part of the subtropic high and blows to China, is weakened also.

An abnormal northwest air stream dominates over East China Sea and the southern China, so the southeast air stream controling these regions in control experiment is weakened obviously. For this reason, the water vapor amount transported to China from the Pacific decreases. An abnormal easterly appears over the southwestern China and the Indo–China Peninsula, this indicates that the component of the southwest monsoon controling these regions in summer, is weakened obviously. In order to make further studies on the effects of the albedo variation due to deforestation in China on the summer monsoon, we analyse the differences of wind vector and speed at 1000 hPa between the sensitive and control experiment (figure omitted). The results show that either the southwest monsoon or the southeast monsoon is weakened obviously after the increasing of the albedo in China.

In the control experiment, at 200 hPa, the southeast part of the anticyclone over the Qinghai–Xizang Plateau prevails with the northeast air stream, part of which crosses the equator, and subsides over the southern Indian Ocean, and then turns into the southeast trade wind near surface layer and at last forms a vertical meridional cell called the monsoon circulation cell. It is shown from Figs.5a,b that the upper cross–equatorial flow, the subsidence air flow over the Indian Ocean as well as the southwest air flow near the surface layer all are weakened obviously. Therefore, the monsoon circulation cell is weakened. The results discussed above show that the increasing of the albedo in China due to the deforestation exerts remarkable effects on the circulations not only over China but also over its neighboring regions.

2. *Influences of the Variations of Albedo on the Climate in China*

Comparing the sensitive experiment with the control experiment, we study the effects of the deforestation on the climate in China.

The difference of the precipitation between the control experiment and the sensitive experiment is shown in Fig.6. The results show that the precipitation decreases in the most part of China, except for a small part of China. The similar result is also obtained in the other simulations for the variations of albedo. J. Lean et al. (1989) studied the effects of the deforestation in the Amazon valley on the climate, and found that the rainfall in the Andes increased unusually. The precipitation in the three rainfall belts greatly decreases, they are the rainfall belts in North China, the southwestern China and South China. The decrement of precipitation is about 6–10 mm / day. This shows that the rainfall in China is very sensitive to the change of albedo. With the weakening of the lower–layer convergences and the upper–layer divergences, the ascending motion in China is weakened. Consequently, the increasing of albedo destroys two important conditions of rainfall formation, and then leads to the decreasing of the precipitation.

The difference of cloud amount between the sensitive experiment and control experiment is shown in Fig. 7. We can see that the cloud amount over the most part of China reduces, especially in the central and west part of China.

The difference of evaporation is shown in Fig. 8. The values in Fig. 8 are enlarged by ten times. It is found that the variations of evaporation are very small. That is to say, the change of albedo has a very weak influence upon evaporation. This result is in coincidence with that of the other experiments carried out by many scientists.

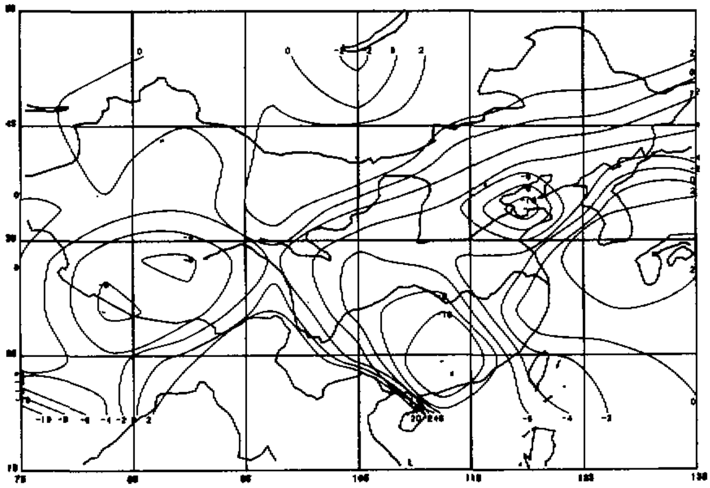

Fig. 6. The difference of the rainfall in China between the sensitive and control experiment.

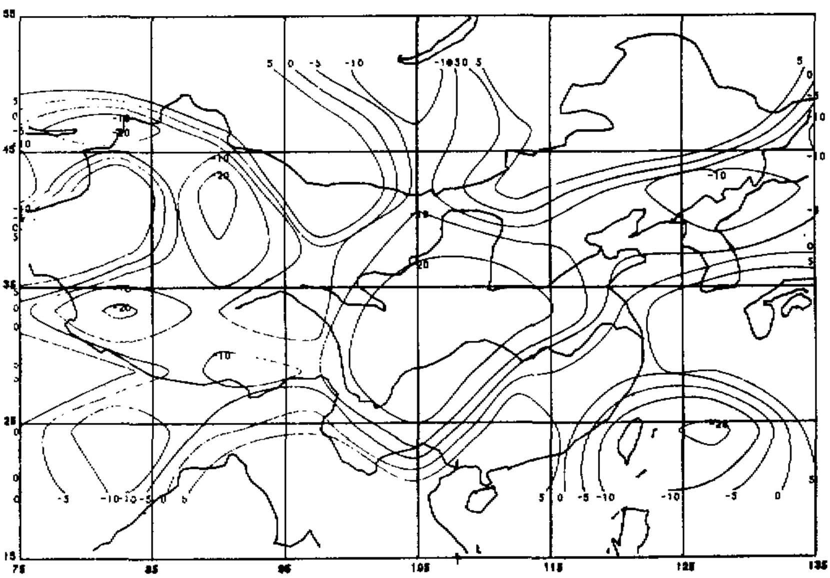

Fig. 7. The difference of the cloud in China between the sensitive and control experiment.

In order to make a summary, the effects of the albedo on the climate in China are shown in Table 2. The averaged precipitation in China decreases by 1.9 mm / day, 25.2% less than that in the control experiment. The averaged evaporation in China decreases by 0. 35

mm / day. Therefore, the increasing of albedo results in the great decrement in the local precipitation and the convergence water vapour flux. Although the evaporation reduces slightly, the drought in China due to the deforestation is serious.

Table 2. Summary of the Difference in Surface Variable for Increased Albedo from Control Simulation

Surface variable	Control experiment	Sensitive experiment	Difference	Percent
Precipitation (mm / d)	7.54	5.64	−1.90	−25.2%
Evaporation (mm / d)	4.19	3.84	−0.35	−8.4%
P−E (mm / d)	3.35	1.80	−1.55	−46.2%
Temperature(°C)	21.40	21.59	0.19	0.88%

V. CONCLUSIONS

1) The NCAR CCM0B Model can simulate the summer climate in China and its neighboring regions very well.

2) After the increasing of albedo due to the deforestation in China, the upper−layer anticyclonic circulations and the lower−layer cyclonic circulations over China are weakened, so the local ascending motion is decreased.

3) Because the summer monsoon is weakened, the water vapor amount transported into China decreases. The north branch of the upper easterly jet weakens, while its south branch strengthens. This kind of variation of the easterly jet will make the ITCZ over South China Sea strengthen.

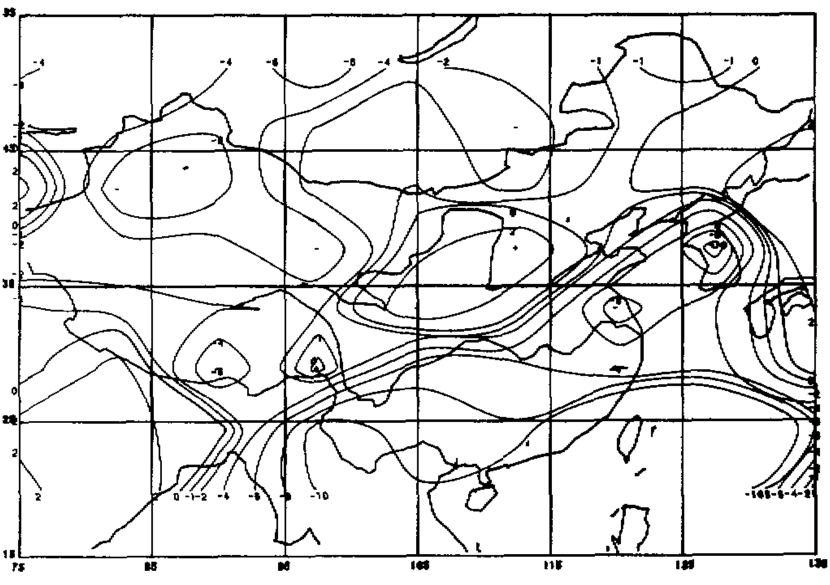

FIG 8 ALBB-CTL 7TH MONTH CHINA EVAPORATION *10.0

Fig. 8. The difference of the evaporation x10 in China between the sensitive and control experiment.

4) Because the ascending motion and the water vapor amount transported into China are decreased, the precipitation is diminished obviously, especially in the three rainfall belts. But its influence on the drought is different in different regions. In North China, the precipitation decreases, and the evaporation increases, so the soil humidity decreases, this will result in the drought. In South China, the rainfall decreases heavily, but the variation of the evaporation is small, so the soil humidity decreases slightly and will result in the slight aridity. In the southwestern China, the precipitation decreases, and the evaporation decreases also (but increases in a few regions), that will lead to the severe drought.

5) The increasing of albedo due to the deforestation in China has remarkable influences on the climate not only in China but also in Asia.

From the above-mentioned discussion, we find that the numerical experiment is successful for studying the impacts of the deforestation on the climate by use of the CCM0B model. However, the physical scheme of surface process in the model is not perfect without a biosphere process, so we only take one vegetation parameter into account to influence the atmospheric circulations, that was the albedo. In the future, with improved model and increased confidence in the modelling of physical processes, a better assessment of the local, regional and global implications of deforestation can be made.

REFERENCES

Atlas of Land Resources in China, 1990 CISNAR.

Atlas of the People's Republic of China, 1989, the Chinese Cartological Publishing Hourse.

Charney, J. (1975a), Dynamics of deserts and drough in the Sahel, in the physical Basis of climate and climate modelling, WMO-ICSU, GARP. Publication Series O. **16:** 171-176.

Charney, J. (1975b), Dynamics of deserts and drought in the Sahel, *Quarterly Journal of the Royal Meteorological Society*, **101:** 193-202.

Charney, J. Quirk, W.J., Chow, S.-H. and Kornfield (1977), A comparative study of the effects of albedo change on drought in semi-arid regions, *Journal of the Atmospheric Sciences*, **34:** 1366-1385.

Dickinson, R.E. and Henderson-sellers, A. (1988), Modelling Tropical Deforestation: A study of GCM land surface parameterizations, *Q. J. R. Meteorol. Soc.*, **114:** 439-462.

Dickinsion, R.E. (1987), Introduction to Vegetation and Climate Interactions in the Humid Tropics, The Geophysiology of Amazonia 3-10. Wiley, New York.

Divid L. Williamson (1989), Description of NCAR Community climate Model(CCM0B).

Dong Min and Shao Yongning et al. (1990), A study of the mean atmospheric circulation in the tropics, *Journal of Tropical Meteorology*, Vol.6, No. 3 227-238 (in Chinese).

Elaine Mathews (1985), Atlas of Archived vegetation, Land-use and Seasonal Albedo data sets, Technical Memorandum 86199.

J. Lean and D. A. Warrilow (1989), Climatic impact of Amazon deforestation, *Dynamical Climatology*, July.

Otterman, J.(1974), Baring height-albedo soils by overgrazing: A hypothesized desertification mechanism, *Science*, **186:** 531-533.

Suel, Y.C. and Fennessy, M.(1982), A study of the influence of surface albedo and July circulation in semi-arid regions using the GLAS GCM, *Journal of climatology*, **2:** 105-125.